Supplementary Information

Facile Synthesis of Starch-Based Nanoparticles Stabilized Pickering Emulsion: Its pH-Responsive Behavior and Application for the Recyclable Catalysis

Liang Qi[1], Zhigang Luo[1,2,3*], Xuanxuan Lu[4]

1. School of Food Science and Technology, South China University of Technology, Guangzhou 510640, China

2. Overseas Expertise Introduction Center for Discipline Innovation of Food Nutrition and Human Health (111 Center), Guangzhou 510640, China

3. Guangdong Province Key Laboratory for Green Processing of Natural Products and Product Safety, South China University of Technology, Guangzhou 510640, China

4. Department of Food Science, Rutgers, The State University of New Jersey, 65 Dudley Rd, New Brunswick, New Jersey 08901, USA

[*]Corresponding author:

Zhigang Luo, Tel: +86-20-87113845, Fax: +86-20-87113848. *E-mail address*: zhgluo@scut.edu.cn

Figure S1. ^{13}C NMR spectra of starch-based nanoparticle with various DMAEMA grafting.

Figure S2. Photographs of Pickering emulsions stabilized by starch-based nanoparticles treated with pH 9 and pH 3 after 5 min.

Figure S3. In-time optical micrographs of droplets in the D-g-SNP stabilized emulsion at pH 7.

Figure S4. Evolution of the surface coverage and emulsion index of D-g-SNP stabilized emulsion (0.3 wt %, pH 9) as a function of storage time.

Figure S5. Size distribution and average size of droplets in stabilized Pickering emulsion (1st, 2nd, 4th and 8th cycle)

Figure S6. SEM images of D-g-SNP treated with pH 3,7 and 9.

Figure S7. Rheological characterization of D-g-SNP dispersions and D-g-SNP stabilized ethyl acetate-water emulsions prepared with different NaCl concentrations: shear stress versus shear rate; viscosity versus shear rate.

Figure S8,9. Photographs of successive pH-responsible D-g-SNP stabilized Pickering emulsion inversion using ether, n-butanol, n-hexane and petroleum ether as the oil phase.

Figure S10. Gas chromatograms of (a) p-nitroaniline and (b) p-anisidine and fitted standard curve.

Figure S11. Real-time data of Gas chromatograms in the p-nitroanisole hydrogenation catalyzed by D-g-SNP/AuNP under different conditions.

Table S1. Element composition and calculated nitrogen composition of monomers in starch-based nanoparticles

Table S2. Hydrogenation results of p-nitroanisole in D-g-SNP/AuNP stabilized Pickering emulsion using other organic solvent as oil phase.

Calculation of ω_{DMAEMA}

Because of the limited grafting ratio, we assumed the mass of nanoparticle was the same before and after the BIS grafting. Therefore, based on the area of protons, it was easy to calculate the mass ratio of DMAEMA (ω_{DMAEMA}), according to the eq S1:

$$\omega_{DMAEMA} = \frac{\frac{157 \cdot A}{162 \cdot 6B}}{1 + \frac{157 \cdot A}{162.6B}} \cdot 100\% \quad \text{(S1)}$$

where A is the sum of areas of methyl protons at 2.2 ppm; B is the sum of areas of H-1 proton for anhydroglucose unit; 157 is the molecular weight of the DMAEMA; 162 is the molecular weight of the anhydroglucose unit.

Calculation of ω_{BIS} and n_{DMAEMA}/n_{BIS}

Table S1. Element composition and calculated nitrogen composition of monomers in starch-based nanoparticles

Sample	ω(%)					
	C	H	S	N	N-DMAEMA	N-BIS
SNP	39.49	7.17	0.00	0.02	0	0
SNP-BIS	39.89	7.20	0.00	0.11	0	0.09
SNP-BIS-DMAEMA-1	40.02	7.33	0.00	0.16	0.05	0.09
SNP-BIS-DMAEMA-2	40.92	7.43	0.00	0.36	0.26	0.08
SNP-BIS-DMAEMA-3	40.82	7.42	0.00	0.38	0.28	0.08
SNP-DMAEMA	39.73	7.21	0.00	0.03	0.01	0

The characteristic peaks at 6.0-6.2 ppm should be the protons in H_2C=CH-for BIS, but they were always too vague to identify from 1H NMR due to the trace amount.[1] Meanwhile, the areas of the multiple hydrogen atoms could not be used in the quantitative calculation. For this reason, the elementary analysis was conducted as an assistance for detecting the mass ratio of total nitrogen content in the samples (ω_N), according to the previous reports[2, 3]. As shown in Table S1, the increase in ω_N from

0.02% to 0.38% was due to the various degrees of monomer grafting, thus approximately mass ratios of nitrogen content for monomers (sum of $\omega_{N\text{-}DMAEMA}$ and $\omega_{N\text{-}BIS}$) were determined according to the difference in the nitrogen content before and after grafting. Based on that, the mass ratio of BIS (ω_{BIS}) and the molar ratio of DMAEMA to BIS (n_{DMAEMA}/n_{BIS}) were determined as follows and shown in Table 2.

$$\omega_{N-DMAEMA} = \frac{14}{157}\omega_{DMAEMA} \tag{S2}$$

$$\omega_{N-BIS} = \omega_N - 0.02 - \omega_{N-DMAEMA} \tag{S3}$$

$$\omega_{BIS} = \omega_{N-BIS} \cdot \frac{154}{2 \cdot 14} \tag{S4}$$

$$n_{DMAEMA}/n_{BIS} = \frac{154 \cdot \omega_{DMAEMA}}{157 \cdot \omega_{BIS}} \tag{S5}$$

where 154 is the molecular weight of the BIS; 14 is the molecular weight of the nitrogen atom.

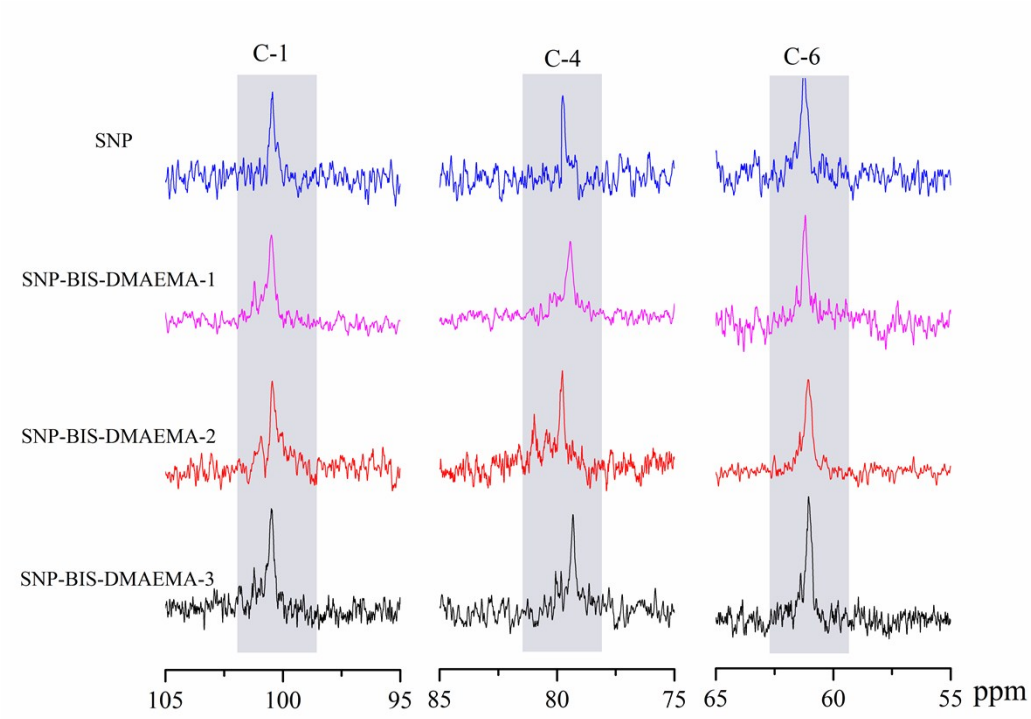

Figure S1. ^{13}C NMR spectra (105-95, 85-75, 65-55 ppm) of starch-based nanoparticle with various DMAEMA grafting

The C-1 of glucose in the α-1,4-repeat units of starch appears at around100 ppm.[4] The C-1 signals of the internal glucosyl units of starch-based nanoparticle with various DMAEMA grafting (SNP-BIS-DMAEMA-1 to 3) became broader than those of pristine starch-based nanoparticle (SNP) in **Figure S1**, suggesting that the substitution occurred at O-2 and that the O-2 substituent affected the chemical shift of the neighboring C-1.[4] Moreover, additional resonances were noted at 80-81 ppm, the resonance from C-4 of internal glucosyl units in starch suggesting that monomers were substituted at the neighboring O-3 position in starch-based nanoparticle.[4,5] Interestingly, no obvious changes was observed in the signal at 60-62.5 ppm, which arose from C-6. We concluded that substitution mainly occurred at O-2 and O-3 and not at O-6.

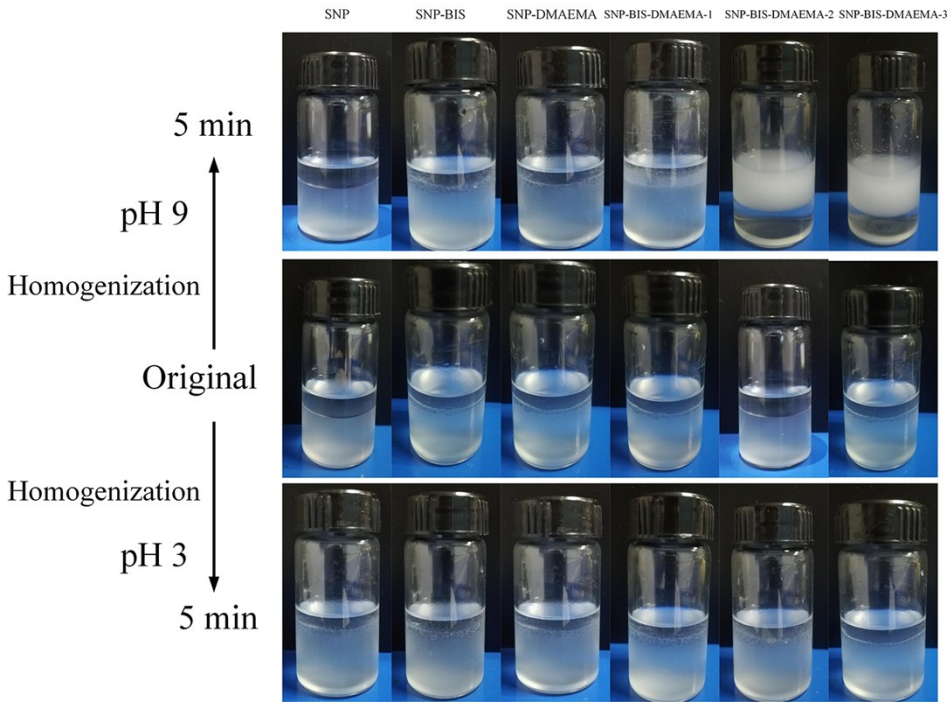

Figure S2. Photographs of Pickering emulsions stabilized by starch-based nanoparticles treated with pH 9 and pH 3 after 5 min.

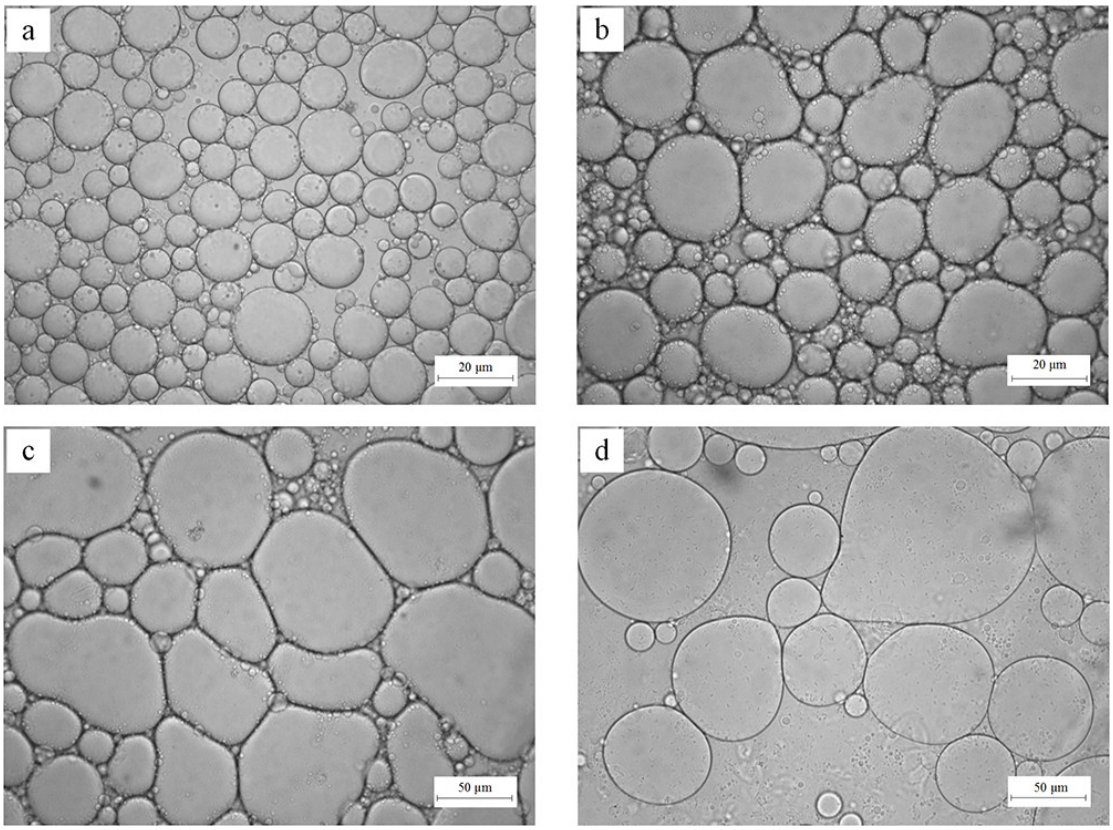

Figure S3. In-time optical micrographs of droplets in the D-g-SNP stabilized emulsion at pH 7 (a:1min, b:5min, c:10min, d:20min).

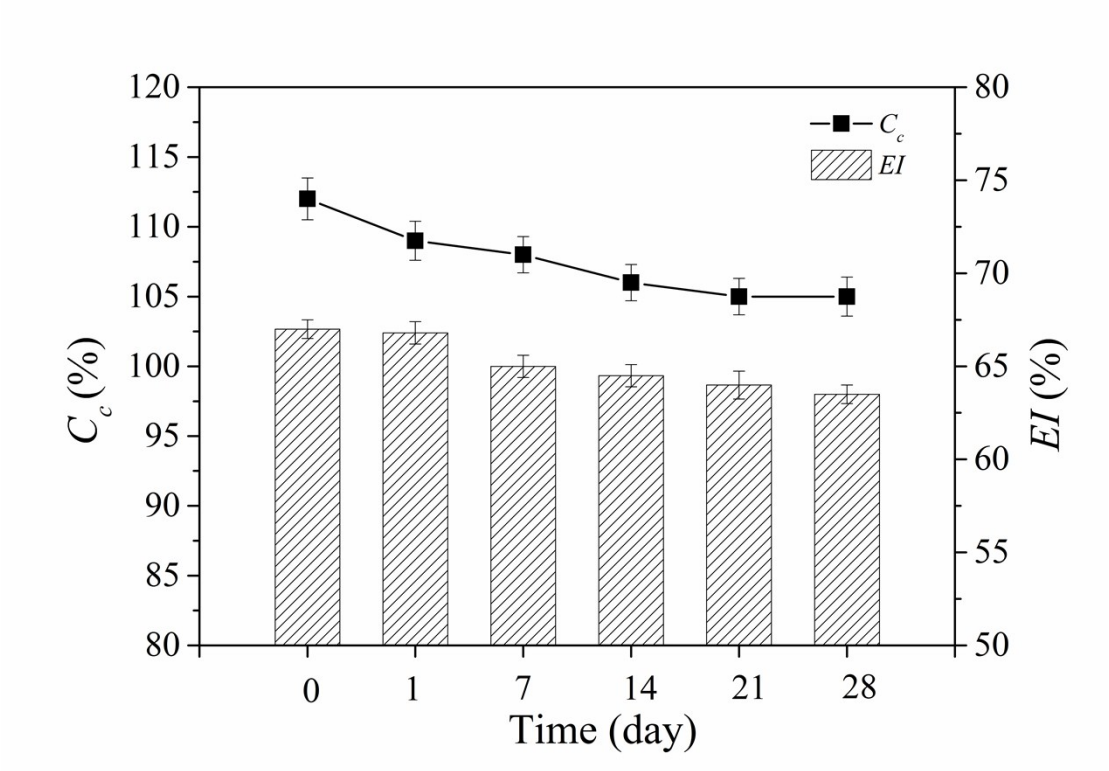

Figure S4. Evolution of the surface coverage and emulsion index of D-g-SNP stabilized emulsion (0.3 wt %, pH 9) as a function of storage time.

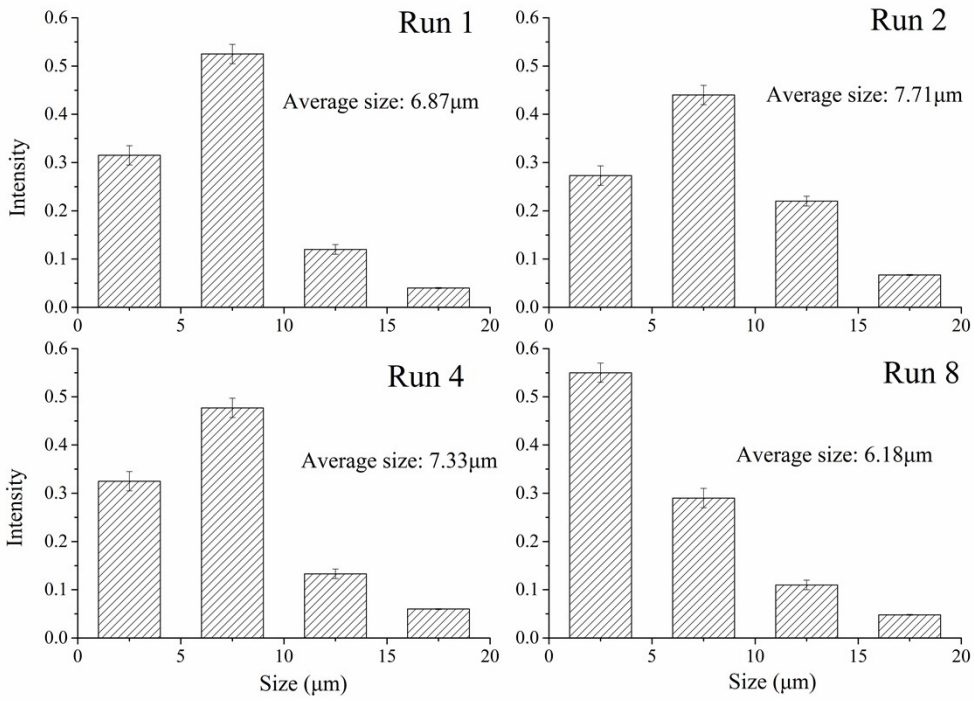

Figure S5. Size distribution and average size of droplets in stabilized Pickering emulsion (1st, 2nd, 4th and 8th cycle)

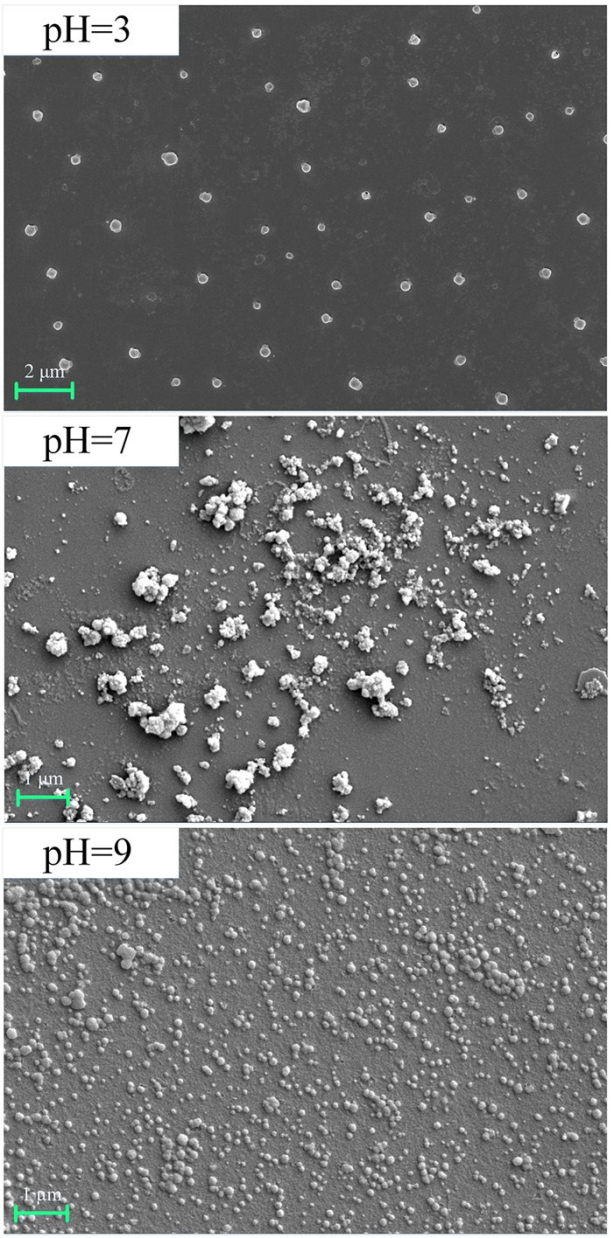

Figure S6. SEM images of D-g-SNP treated with pH 3,7 and 9.

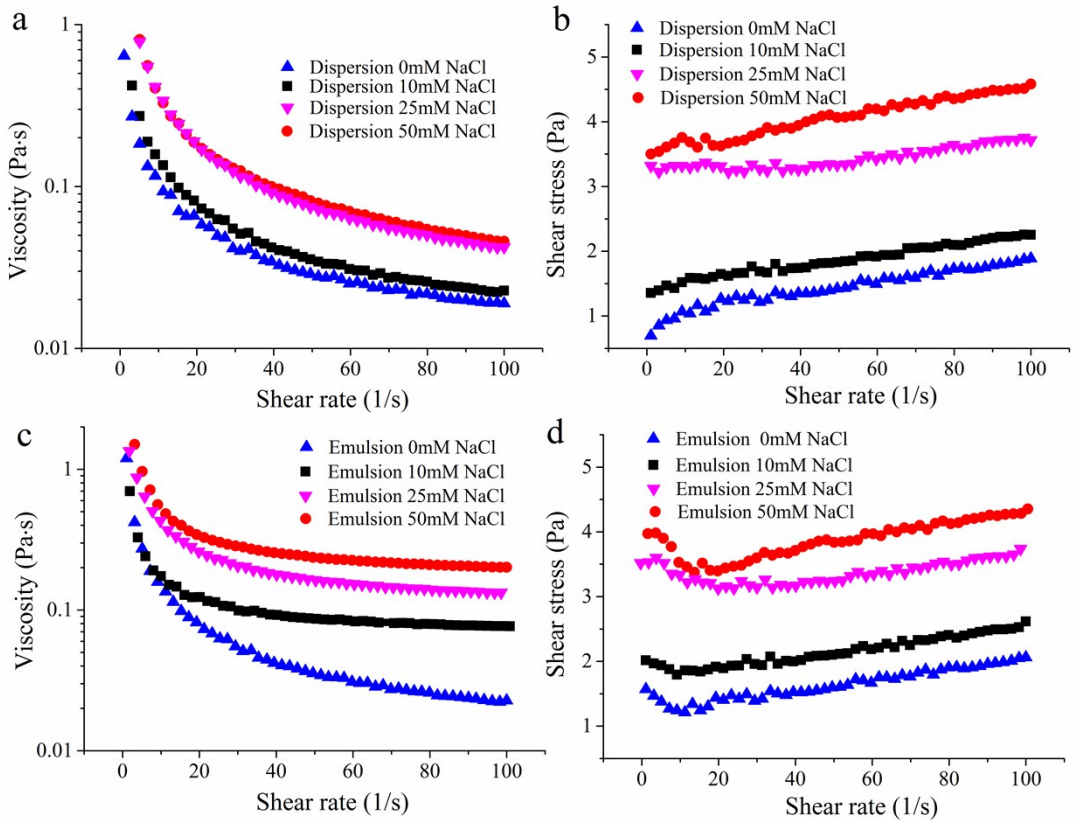

Figure S7. Rheological characterization of D-g-SNP dispersions (a, b) and D-g-SNP stabilized ethyl acetate–water emulsions (c, d) prepared with different NaCl concentrations: (a, c) shear stress versus shear rate; (b, d) viscosity versus shear rate. The pH value of water was 9.

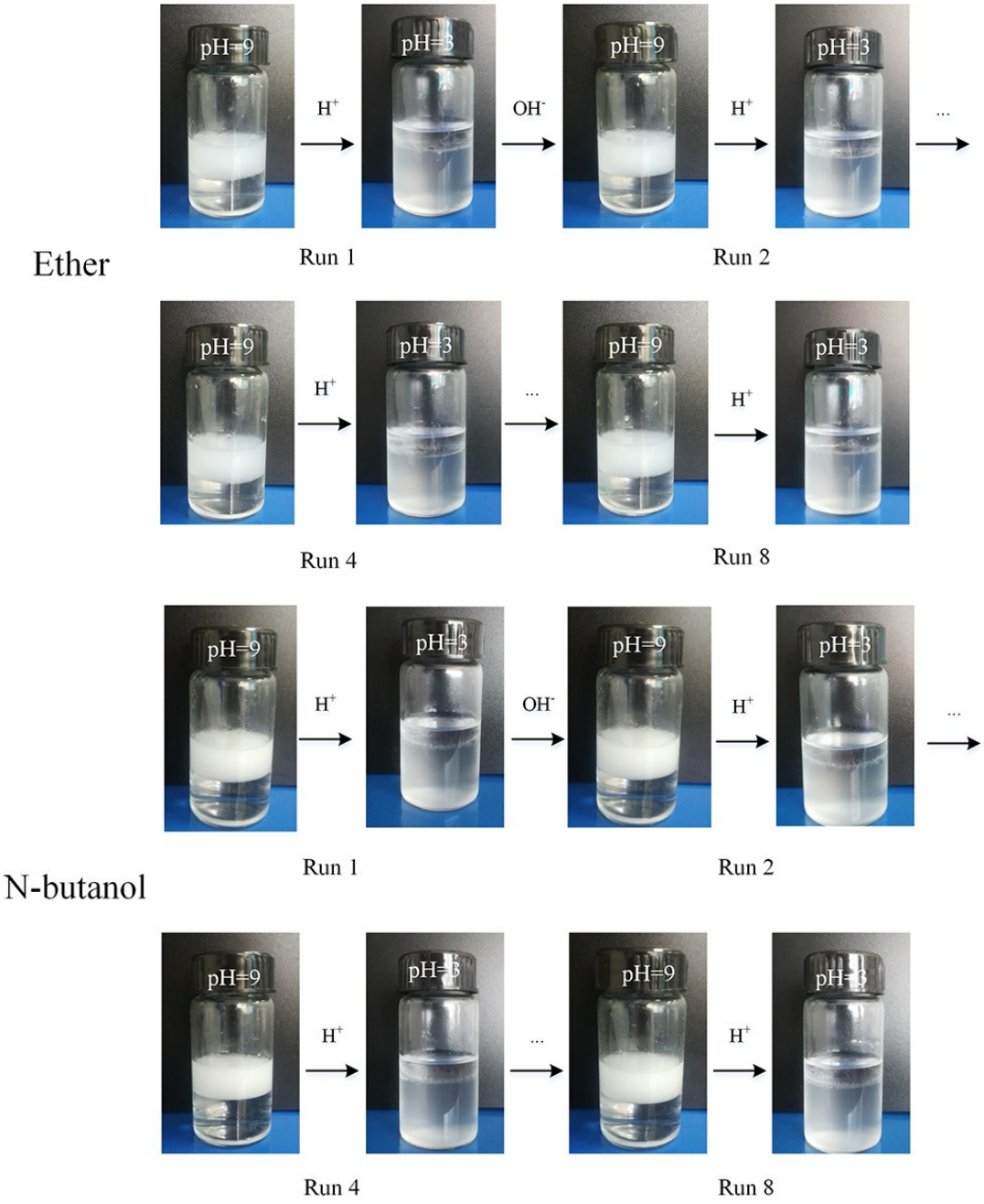

Figure S8. Photographs of successive pH-responsible D-g-SNP stabilized Pickering emulsion inversion using ether or n-butanol as the oil phase (1st, 2nd, 4th and 8th cycle)

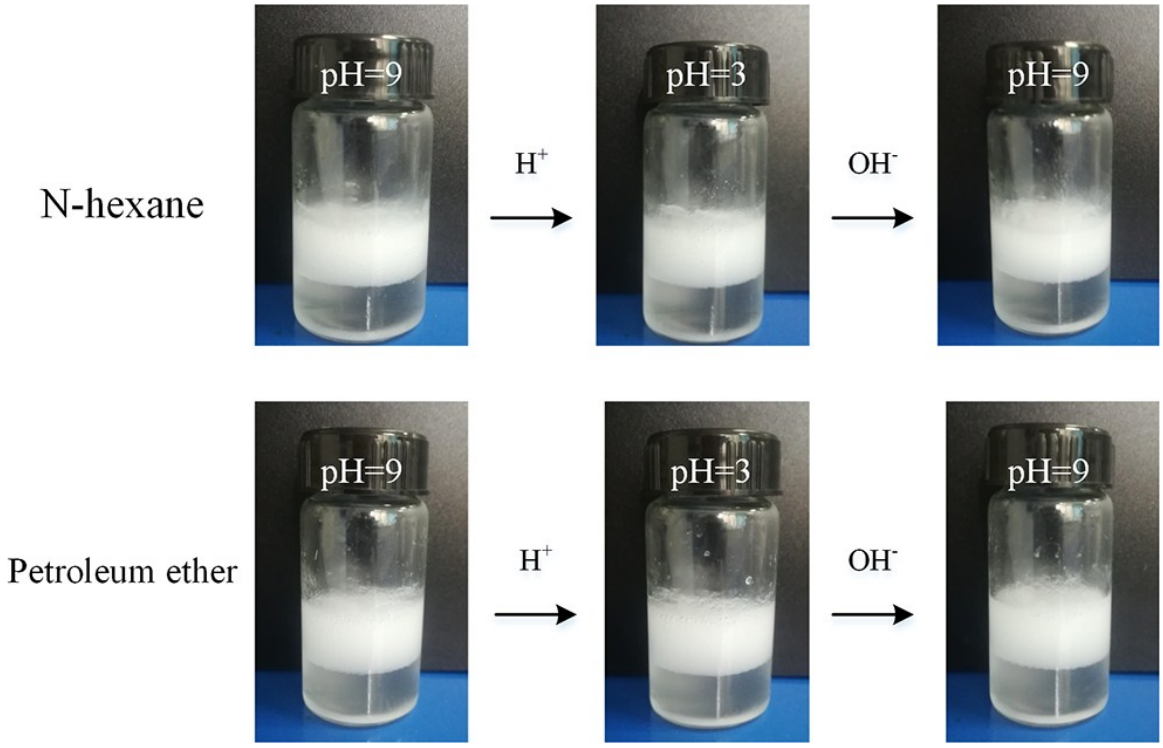

Figure S9. Photographs of successive pH-responsible D-g-SNP stabilized Pickering emulsion inversion using n-hexane and petroleum ether as the oil phase

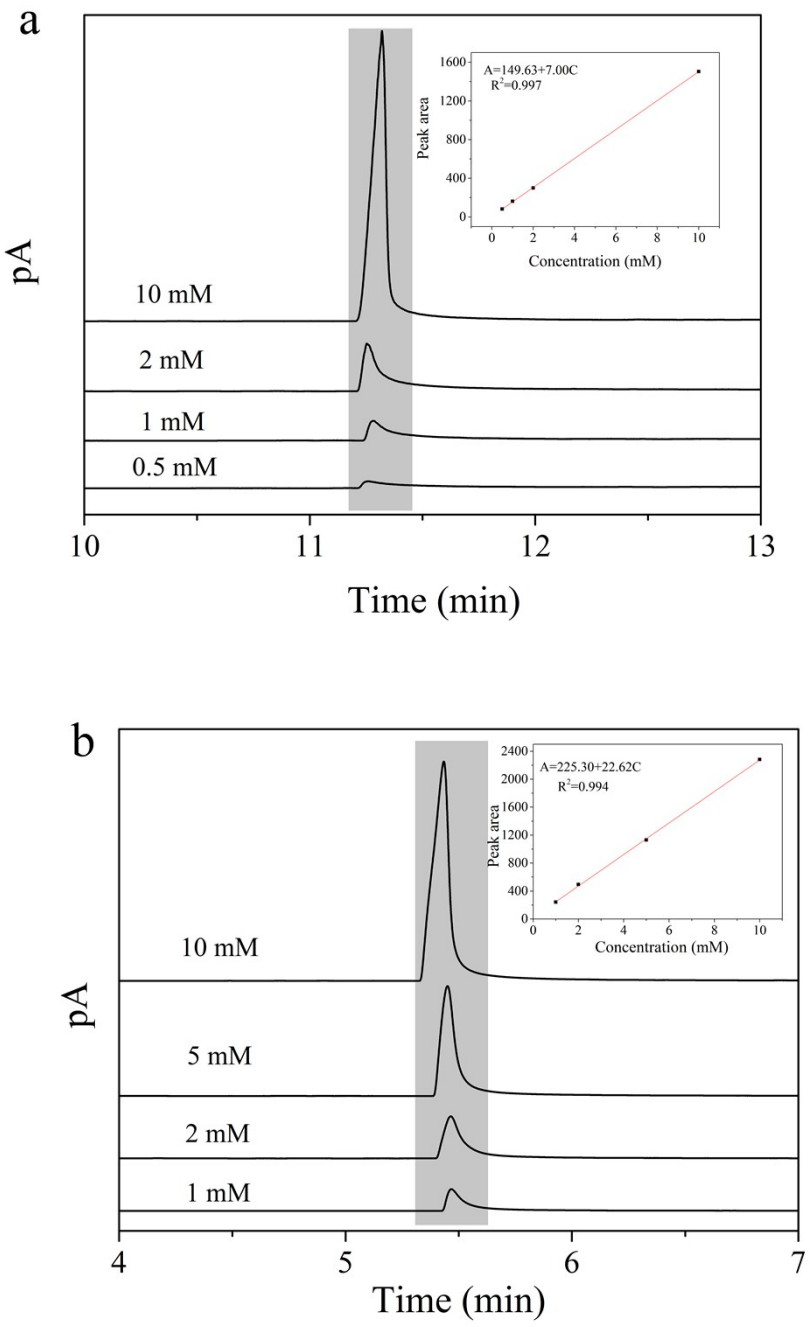

Figure S10. Gas chromatograms of (a) p-nitroaniline and (b) p-anisidine and fitted standard curve.

We prepared two standard solutions in different concentrations, and obtained two standard chromatograms. The linear relation between peak areas and concentrations was fitted and characterized by the regression equation as inserted photograph. The accuracy of this equation could be quantified by correlation coefficient, which was

higher than 0.99. From the chromatogram of catalysis reaction, the amount of aromatic nitro-/amino- compounds could be measured through peak area (in grey shadow zone). In virtue of regression equation, the concentration of aromatic nitro-/amino- compounds could be readily figured out. The calculation of yield was based on:

$$Yield = Conversion\ rate\ (\%) \cdot Selectivity\ (\%) \quad \text{(S6)}$$

where the conversion rate is the ratio of substrates that are involved in the reaction to the whole number of substrates, while selectivity is the ratio of desired products to the whole number of obtained products.

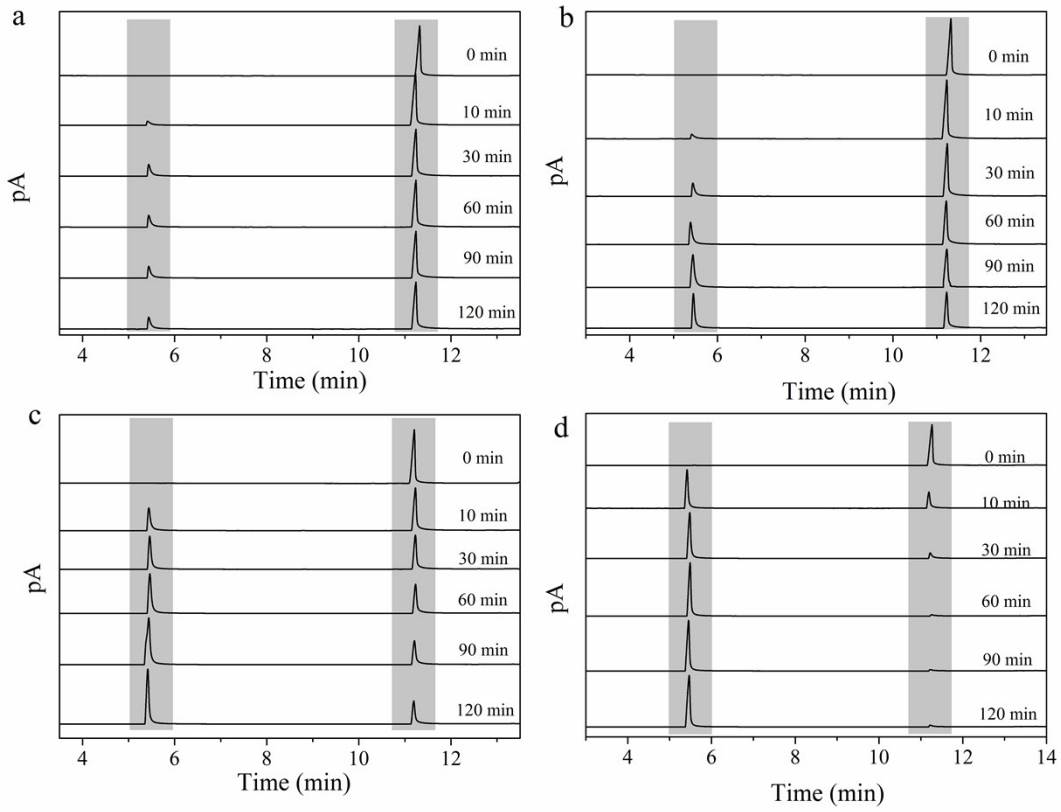

Figure S11. Real-time data of Gas chromatograms in the p-nitroanisole hydrogenation catalyzed by D-g-SNP/AuNP under the (a) monophase system, (b) planar interface system with 300rpm and (c) 900rpm, as well as (d) Pickering emulsion system.

Table S2. Hydrogenation results of p-nitroanisole in D-g-SNP/AuNP stabilized Pickering emulsion using other organic solvent as oil phase.

Organic solvents	Run1		Run2		Run4		Run8	
	Time(h)	Yield(%)	Time(h)	Yield(%)	Time(h)	Yield(%)	Time(h)	Yield(%)
Ether	1.5	96.3	1.5	95.3	1.5	92.3	1.5	87.2
N-butanol	2	97.2	2	96.2	2	93.2	2	86.9

References for Supporting Information:

1. Garcıa, D.; Escobar, J.; Bada, N.; Casquero, J.; Hernáez, E.; Katime, I., Synthesis and characterization of poly (methacrylic acid) hydrogels for metoclopramide delivery. *European polymer journal* 2004, 40, 1637-1643.

2. Kan, K. H. M.; Li, J.; Wijesekera, K.; Cranston, E. D., Polymer-Grafted Cellulose Nanocrystals as pH-Responsive Reversible Flocculants. *Biomacromolecules* 2013, 14, 3130-3139.

3. Tang, J.; Lee, M. F. X.; Zhang, W.; Zhao, B.; Berry, R. M.; Tam, K. C., Dual responsive pickering emulsion stabilized by poly [2-(dimethylamino) ethyl methacrylate] grafted cellulose nanocrystals. *Biomacromolecules* 2014, 15, 3052-3060.

4. Bai, Y.; Shi, Y. C.; Herrera, A.; Prakash, O., Study of octenyl succinic anhydride-modified waxy maize starch by nuclear magnetic resonance spectroscopy. *Carbohydrate Polymers* 2011, 83, 407-413.

5. Hui, C.; Xu, K.; Wu, X.; Qiang, C.; Xue, D.; Song, C.; Zhang, W.; Wang, P., Effect of acetylation on the properties of corn starch. *Food Chemistry* 2008, 106, 923-928.